JOURNAL OF MATERIALS SCIENCE 22 (1987) 3698–3702

D.c. conduction in thin films of SiO/In_2O_3 before and after electroforming

Z. T. AL-DHHAN, C. A. HOGARTH
Department of Physics, Brunel University, Uxbridge, Middlesex UB8 3PH, UK

Electrical measurements on thin co-evaporated SiO/In_2O_3 films before and after electroforming are reported. The high-field conduction (expressed in terms of circulating current I_c and bias voltage V_b) in thin film sandwich structures of $Al-SiO/In_2O_3-Al$ and $Cu-SiO/In_2O_3-Cu$ is found to obey a relation of the form $\log I_c \propto V_b^{1/2}$. The electroformed samples show voltage-controlled negative resistance, voltage memory, thermal–voltage memory and pressure–voltage memory effects and the results are explained in terms of the filamentary model of electrical conduction.

1. Introduction

An amorphous high-resistivity semiconductor or a dielectric material sandwiched between two electrodes can show such properties as memory switching, and for this an amorphous material is normally used whose structure can be changed reversibly between two structural states; the amorphous state which generally has a high resistance and a microcrystalline state which has a reduced resistance [1]. The electrical properties of thin oxide films are of current interest partly because some behave as good dielectric materials while others make transparent conducting materials and there is continued interest in novel materials for those purposes. In_2O_3 is normally regarded as a reasonably highly-conducting oxide and little if any information is available about its properties when mixed with SiO in amorphous thin film form. A number of models have been suggested to account for the forming process and related phenomena and these have been discussed in a comparative way by Ray and Hogarth [2]. The preferred model is the polyfilamentary model, which was first proposed by Dearnaley [3] and was extended by Ralph and Woodcock [4] and by Rakhshani *et al.* [5] and has had considerable success in explaining the various electrical properties of the electroformed devices.

Some studies of electron spin resonance and optical absorption edge in amorphous mixed films of SiO and In_2O_3 were presented earlier by Arshak *et al.* [6].

2. Experimental work

Films were prepared by a technique of thermal co-evaporation as described by Hogarth and Wright [7] in a Balzers BA 510 coating unit and deposited on clean Corning 7059 (2.54 cm × 7.62 cm) substrates, as successive layers of metal–insulator–metal (MIM) at pressures of about 6×10^{-6} torr with a substrate temperature of $\approx 100°$ C. The warming of the substrate improved the adhesion of the thin films. Tantalum and molybdenum boats were used for the evaporation of SiO and In_2O_3, respectively. The thickness of each of the films was monitored using a quartz crystal monitor. Six samples were deposited on each substrate with a common base electrode. Each device had an active area of 0.15 cm^2. Fig. 1 shows the arrangement of the samples. Conventional methods were used to make d.c. electrical measurements in a subsidiary vacuum system at a pressure of 10^{-6} to 10^{-5} torr. The d.c. bias voltage was provided by a Coutant LA 100.2 power supply and the current was recorded by an electronic avometer. The voltage across the sample was monitored by a digital voltmeter. Lowering of the sample temperature was achieved by firmly attaching it to the brass base fitted to a stainless steel tank containing liquid nitrogen. Heating the sample above room temperature was initiated by using a resistive heater inserted in holes made through the brass base. Sample temperatures were monitored by a Comark electronic thermometer.

3. Results and discussion

3.1. D.C. conduction before electroforming

At low fields ohmic behaviour was always observed in our samples, followed by a non-linear dependence of current on voltage at the higher fields as shown in Figs 2a and b for different electrode materials. The analysis of these results is shown in Figs 3a and b where $\log I_c$ is plotted as a function of $V_b^{1/2}$. This relation is indicative of either Schottky emission [8] or the Poole–Frenkel effect [9]. Both phenomena are described by the relation

$$I_c \propto \exp [\beta E^{1/2}/kT] \quad (1)$$

where I_c is the circulating current, E the mean applied field ($= V_b/d$), d being the insulator thickness, k is the Boltzmann constant, T the absolute temperature and β the field lowering coefficient given by

$$\beta = [e^3/n\pi\varepsilon_0\varepsilon_r]^{1/2} \quad (2)$$

ε_0 is the permittivity of free space and ε_r is the relative permittivity of the dielectric. The difference between these two effects is expressed by $n = 1$ for the Poole–

0022–2461/87 $03.00 + .12

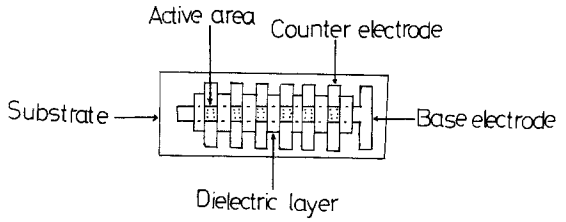

Figure 1 Arrangement of the specimens.

Frenkel effect and $n = 4$ for Schottky emission. The experimental value of β for the systems under investigation lies close to the calculated value of β_s. We may therefore regard the high-field conduction mechanism as being predominantly of the Schottky type. The values of barrier-lowering coefficient β and the relative dielectric constant ε_r calculated in a similar manner to the results of Khan *et al.* [10], are tabulated in Table Ia and b.

Analysis of the high-field conduction has revealed that the Schottky process of conduction was dominant, with activation energy $\Delta E = 0.21$ eV as shown in Fig. 4. At low temperatures between 201 and 296 K, the conductivity was found to be governed by a hopping conduction associated with an activation energy $\Delta E = 0.09$ eV. The transition from hopping conduction to free band conduction was noted at about 23° C.

3.2. Electroforming and voltage controlled negative resistance (VCNR)

In order to electroform a MIM device it was necessary to apply a minimum forming voltage across it for a definite period of time. This minimum voltage was found to be determined not only by the electrode material, but also by the conditions of the insulator. Fig. 5 shows a reproducible V–I characteristic for an Al–80 mol % SiO/20 mol % In_2O_3–Al sample having dielectric thickness of 300 nm and formed by the application of 12 V. The conduction in electroformed samples increased by about 3 orders of magnitude and showed VCNR. The results can be explained on the filamentary model of electrical conduction [3, 11].

TABLE Ia Estimated results for an Al–63 mol % SiO/37 mol % In_2O_3–Al sample (insulator thickness 300 nm)

Temperature (K)	β (eV cm$^{-1/2}$ V$^{-1/2}$)	ε_r
201	7.94×10^{-5}	22.9
297	1.17×10^{-4}	10.6
311	1.22×10^{-4}	9.7
333	1.39×10^{-4}	8.4
373	1.47×10^{-4}	6.7

TABLE Ib Estimated results for a Cu–68 mol % SiO/32 mol % In_2O_3–Cu sample (insulator thickness 300 nm)

Temperature (K)	β (eV cm$^{-1/2}$ V$^{-1/2}$)	ε_r
225	1.77×10^{-4}	4.6
254	1.79×10^{-4}	4.5
297	2.15×10^{-4}	3.1
340	2.43×10^{-4}	2.45
393	2.89×10^{-4}	1.73

3.3. Memory effects

Fig. 6a shows a reproducible V–I characteristic of a sample of composition 37 mol % SiO/63 mol % In_2O_3,

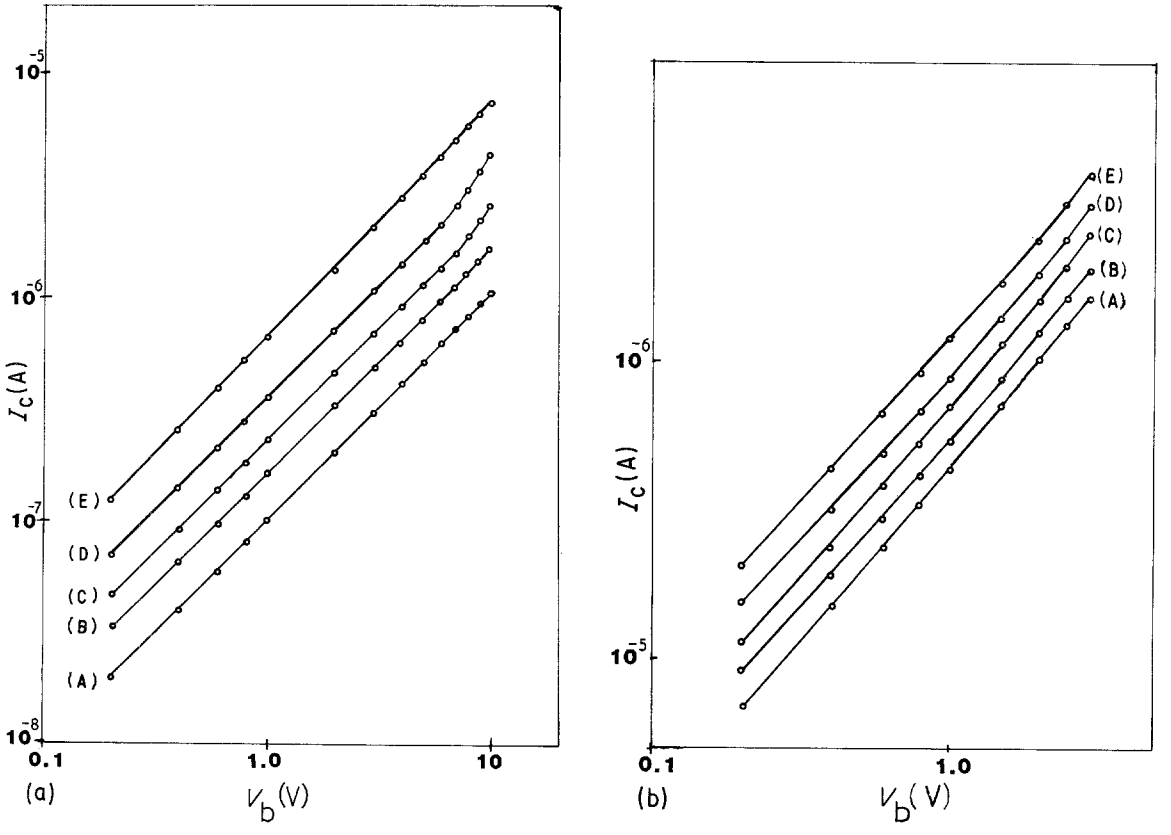

Figure 2 (a) Voltage-current characteristics of a 300 nm thick Al–63 mol % SiO/37 mol % In_2O_3–Al thin film assembly (A) 201 K, (B) 297 K, (C) 311 K, (D) 333 K, (E) 373 K. (b) Voltage–current characteristics of a 300 nm thick Cu–68 mol % SiO/32 mol % In_2O_3–Cu thin film assembly at (A) 225 K, (B) 254 K, (C) 297 K, (D) 340 K, (E) 393 K.

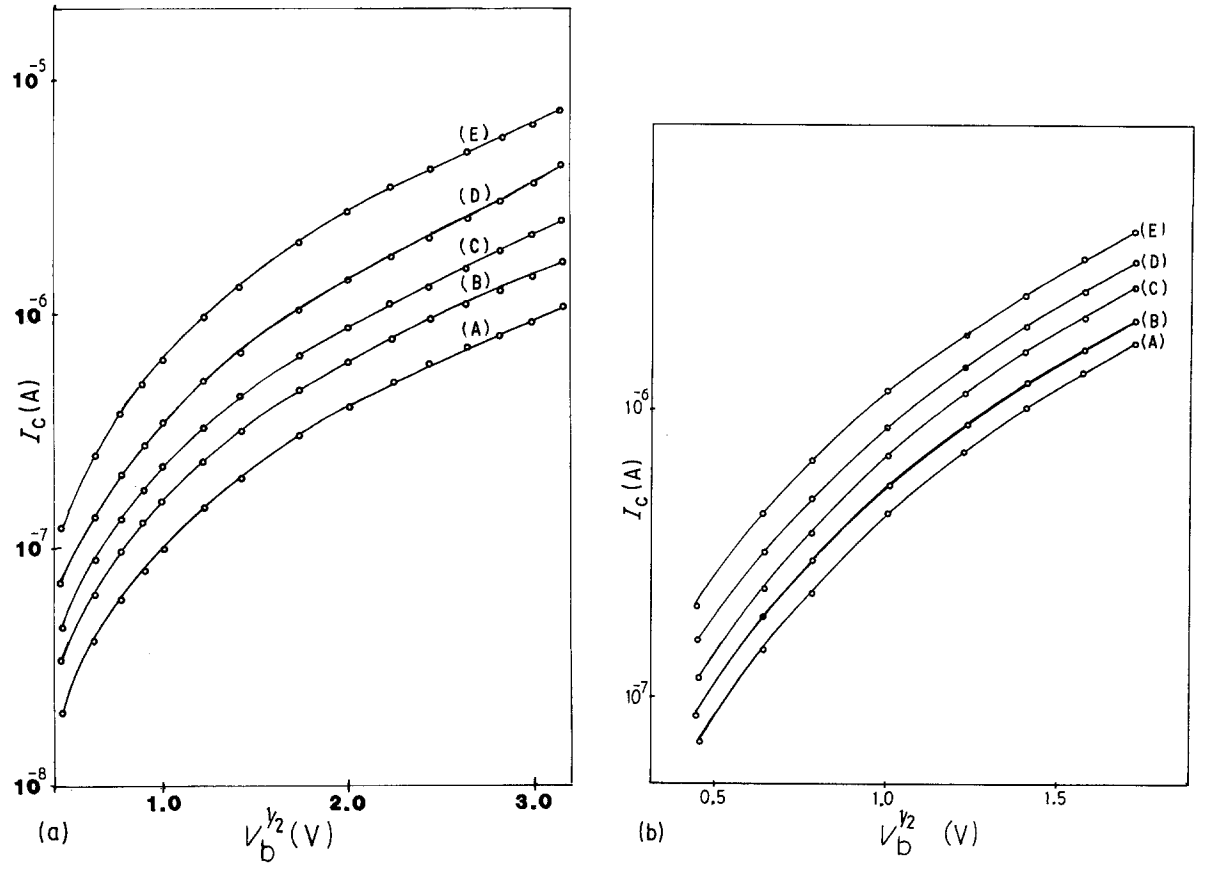

Figure 3 (a) I_c against $V_b^{1/2}$ for a 300 nm thick Al–63 mol % SiO/37 mol % In_2O_3–Al thin film assembly (A) 201 K, (B) 297 K, (C) 311 K, (D) 333 K, (E) 373 K, (b) I_c against $V_b^{1/2}$ for a 300 nm thick Cu–68 mol % SiO/32 mol % In_2O_3–Cu thin film assembly (A) 225 K, (B) 254 K, (C) 297 K, (D) 340 K, (E) 393 K.

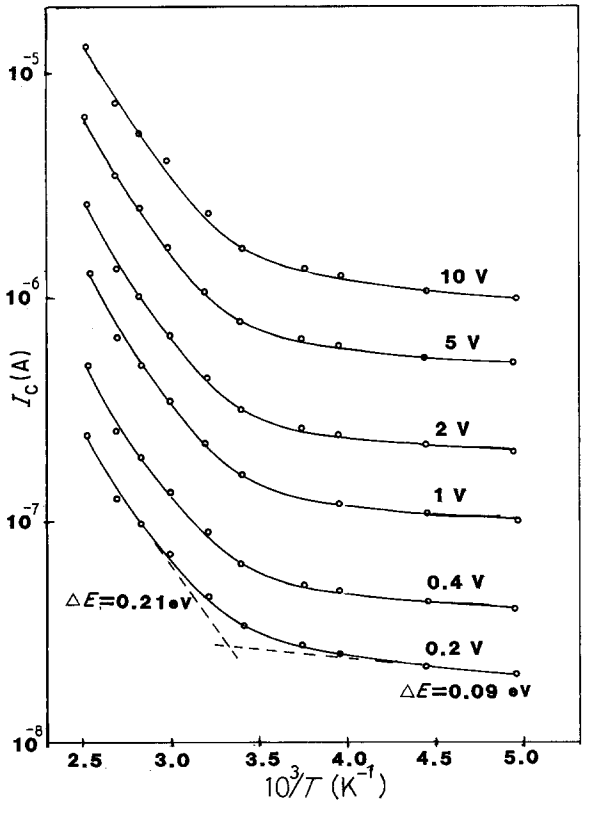

Figure 4 Circulating current as a function of inverse temperature at six applied voltages for an Al–63 mol % SiO/37 mol % In_2O_3–Al thin film assembly. (Bias voltages shown).

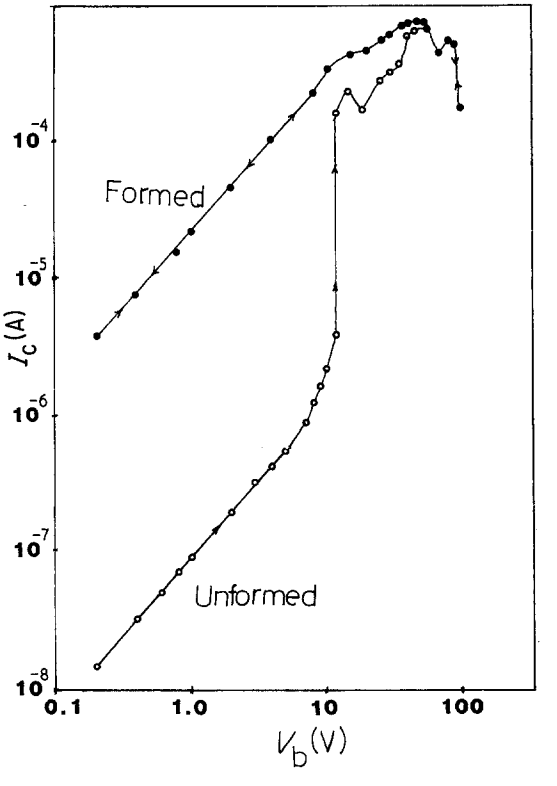

Figure 5 Voltage–current characteristics of a 80 mol % SiO/20 mol % In_2O_3 sample.

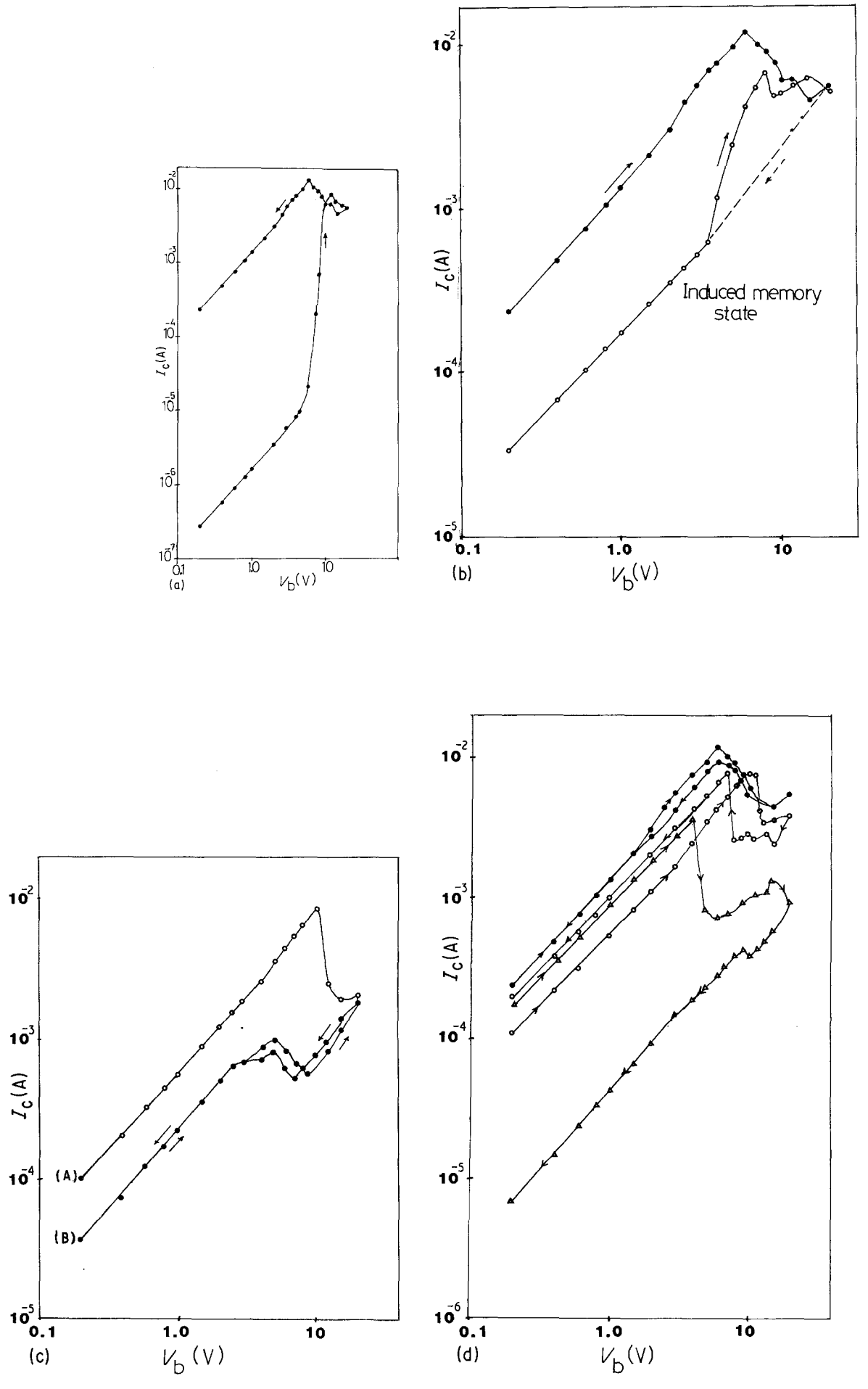

Figure 6 (a) Voltage–current characteristics of a Cu–37 mol % SiO/63 mol % In_2O_3–Cu sample. (b) Curves showing voltage memory effect. Memory state induced at 20 V applied. (c) Curves showing thermal–voltage memory effect at −50° C. (A) first run, (B) further run. (d) Effect of ambient pressure and curves showing a pressure–voltage memory effect in a Cu–37 mol % SiO/63 mol % In_2O_3–Cu sample. (●) 1×10^{-6} torr, (○) 4×10^{-4} torr, (△) 760 torr.

having a thickness of ≈ 300 nm and with 50 nm thick copper electrodes. Initially ohmic behaviour is observed but at 7 V the current increases by 2 orders of magnitude. The new state of the sample is shown in the formed part of Fig. 6a. A voltage memory effect exhibited by the sample at room temperature is shown in Fig. 6b. It was found that a high resistance memory state could be induced if the voltage were lowered rapidly from any point on the VCNR trace to zero, followed by switching off the power supply for a very short time. When a voltage was re-applied the original high resistance state was regenerated up to a particular threshold voltage when the current increased sharply to join up the previous high-conductivity state in the VCNR region. Voltage memory effects are explained by Simmons and Verderber [12] in terms of trapping and release of charges within insulating films, whereas Ralph and Woodcock [4] propose that in the memory state some of the filaments retain sufficient trapped charge to be in the high impedance state.

A thermal–voltage memory effect can also be generated in our samples as shown in Fig. 6c when the sample temperature is reduced to 223 K. The first curve traces the same V–I characteristic as is normally recorded after forming but when the applied voltage is reduced to zero, a highly-resistive memory state is generated and preserved during subsequent measurements of V–I characteristics. Raising the sample to room temperature again develops the low-resistance state, characteristic of an electroformed device. Thermal–voltage memory can also be explained by the model put forward by Dearnaley *et al.* [3].

Pressure–voltage memory effects could also be observed using another procedure involving changes in the ambient atmosphere around the sample which was tested at different ambient pressures as indicated in Fig. 6d. The current passing through the sample was found to follow more or less the same V–I characteristics as measured in a good vacuum (1×10^{-6} torr) with the peak current decreasing as the pressure increased. At atmospheric pressure the current followed the same characteristic up to a certain threshold voltage V_T. Increasing the voltage above V_T caused a decrease in the current and the development of a high-resistance state. This was maintained by reducing the voltage to zero, when the current then assumed a different value depending on the ambient pressure. Increasing the voltage again and then reducing it to zero generated a high-resistance memory state at atmospheric pressure. The high-resistance state could be explained by assuming conduction to take place through the surface states of the mixed oxides expected to be present on the walls of the filaments [13, 14].

References

1. H. FRITZSCHE, "Electronic and Structural Properties of Amorphous Semiconductors", in Proceedings of the Thirteenth session of the Scottish Universities Summer School in Physics, edited by P. G. le Comber and J. Mort (Academic Press, London, New York, 1972) p. 557.
2. A. K. RAY and C. A. HOGARTH, *Int. J. Electronics* **57** (1984) 1.
3. G. DEARNALEY, D. V. MORGAN and A. M. STONEHAM, *J. Non-Cryst. Solids* **4** (1970) 593.
4. J. E. RALPH and J. M. WOODCOCK, *J. Non-Cryst. Solids* **7** (1972) 236.
5. A. E. RAKHSHANI, C. A. HOGARTH and A. A. ABIDI, *ibid.* **20** (1976) 25.
6. K. ARSHAK, C. A. HOGARTH and M. ILYAS, *J. Mater. Sci. Lett.* **3** (1984) 1035.
7. C. A. HOGARTH and L. A. WRIGHT, in Proceedings of the International Conference on Physics of Semiconductors, Moscow (Nauka, Leningrad, 1968) p. 1274.
8. W. SCHOTTKY, *Z. Phys.* **15** (1914) 872.
9. J. FRENKEL, *Phys. Rev.* **54** (1938) 647.
10. M. N. KHAN, M. I. KHAN and C. A. HOGARTH, *Phys. Status Solidi (a)* **61** (1980) 251.
11. G. DEARNALEY, *Thin Solid Films* **3** (1967) 161.
12. J. G. SIMMONS and R. R. VERDERBER, *Proc. Roy. Soc.* **A301** (1967) 77.
13. I. EMMER, *Thin Solid Films* **20** (1974) 43.
14. K. TANAKA, V. UEMURA and M. IWATA, *ibid.* **50** (1978) L25.

Received 17 October
and accepted 27 November 1986